

Center for Quality and Applied Statistics  
Kate Gleason College of Engineering  
Rochester Institute of Technology

# **Stepwise Simplex Projection Method for Selection of Endmembers in Hyperspectral Images**

Peter Bajorski  
Center for Quality and Applied Statistics  
Rochester Institute of Technology  
Peter.Bajorski@rit.edu

Technical Report 2005–1

March 2005





# Stepwise Simplex Projection Method for Selection of Endmembers in Hyperspectral Images

Peter Bajorski

Graduate Statistics Department, Rochester Institute of Technology  
98 Lomb Memorial Drive, Rochester, NY 14623-5604, Email: Peter.Bajorski@rit.edu

## ABSTRACT

In previous research, we introduced a family of simplex projection methods for selection of endmembers in hyperspectral images. In this paper, we define a new member of that family, which we call the Stepwise Simplex Projection (SSP) method. This new method adds and eliminates endmembers based on their distances to simplexes defined by previously chosen endmembers. We compare the SSP method to a previously defined simplex projection method (called the Farthest Pixel Selection method) and to some other methods such as the Pixel Purity Index and Maximum Distance methods. To this end, we introduce several summary measures to describe how well a set of endmembers characterizes the image spectra. We also investigate how well the resulting sets of endmembers perform in subpixel target detection. The numerical results are based on AVIRIS hyperspectral imagery. The SSP method proves to be the most consistently well performing among the investigated methods.

Key Words: MaxD; PPI; simplex projection methods; SSP; FPS; endmembers; AVIRIS; hyperspectral imagery; linear mixing; fully constrained model; subpixel target detection

## 1. INTRODUCTION

It is well known that performance of subpixel target detection algorithms depends on the choice of endmembers used to characterize the background and the target in hyperspectral imagery.<sup>1</sup> The proper choice of endmembers also plays an important role in decomposing the observed hyperspectral scenes (by unmixing procedures) for the purpose of estimating abundances of the present materials.

In previous research,<sup>16</sup> we investigated how well a set of endmembers characterized a given set of spectra, such as background or target regions. We also introduced a family of simplex projection methods for selection of endmembers in hyperspectral images. In this paper, we define a new member of that family, which we call the Stepwise Simplex Projection (SSP) method. This new method adds and eliminates endmembers based on their distances to simplexes defined by previously chosen endmembers. We compare the SSP method to a previously defined simplex projection method (called the Farthest Pixel Selection method) and to some other methods such as the Pixel Purity Index (PPI) and Maximum Distance (MaxD) methods. To this end, we introduce several summary measures to describe how well a set of endmembers characterizes the image spectra.

We are assuming a linear mixing model with coefficients constrained to be positive fractions (between 0 and 1) that sum up to 1. Consequently, for a given set of spectra represented as a set of  $p$ -dimensional vectors (or points), we can define a convex hull (a “region”) generated by convex linear combinations of those vectors. When dealing with a set of background [target] spectra, we will call the convex hull a background [target] region (rather than a background space or subspace, which could be confused with linear spaces).

In the terminology used in <sup>2</sup>, endmembers can be derived from the image (image endmembers) or derived from a library or field reflectance spectra (reference endmembers). Analysis in this article is based on image endmembers. Also, we limit our investigation to the so-called native endmembers (i.e., vectors chosen from within the image spectra).

It is our view that in the target detection methods (which are the focus of this paper), the endmembers do not need to represent pure materials as long as they give a good representation of the background or target regions. It should also be recognized that the concept of a pure material is not always well defined. On the other hand, in the process of unmixing for the purpose of estimating material abundances, the physical interpretation of endmembers becomes more important.

In this paper, the endmember coefficients (abundances) are estimated using the fully constrained least squares method, which is equivalent to projecting on a simplex. We use the projection terminology for ease of geometric and intuitive interpretation.

The four endmember selection methods (considered in this paper) together with the Singular Value Decomposition method (generating basis vectors rather than endmembers) are compared in terms of their target detection performance in Section 5. The numerical results are obtained for an AVIRIS hyperspectral image (100 by 100 pixels) with 152 spectral bands (after the water bands are removed).

## 2. DEFINITIONS

Consider a set of spectra  $\mathbf{x}_i, i=1, \dots, n$ , where  $\mathbf{x}_i$ 's are  $p$ -dimensional vectors (of reflectance or radiance, for example). Such sets may appear in the following contexts:

- A collection of  $n$  pixels in a spectral image
- A collection of target spectra generated under a variety of environmental conditions (such as atmospheric and illumination effects)
- A merged set of the target and image spectra.

It is often convenient to define a relatively small set of spectra  $\mathbf{m}_1, \dots, \mathbf{m}_k$ , called endmembers, such that all  $n$  spectra  $\mathbf{x}_i$  can be represented (at least approximately) as linear combinations of the endmembers, that is,

$$\mathbf{x}_i = \sum_{j=1}^k a_{ij} \mathbf{m}_j + \boldsymbol{\varepsilon}_i \quad (1)$$

where  $a_{ij}$  are constants and  $\boldsymbol{\varepsilon}_i$  are approximation errors (residuals), which can be due to the noise in data or due to modeling error (or both). In the context of a spectral image, the linear combination (1) can be interpreted as representing a mixture of materials (defined by endmembers) contained in the image pixels, and the constants  $a_{ij}$  can be interpreted as abundances of those materials. This is why we are going to assume a convex linear combination in (1), that is,

$$a_{ij} \geq 0 \quad \text{and} \quad \sum_{j=1}^k a_{ij} = 1 \quad (2)$$

which is often called a fully constrained case (e.g., see <sup>5</sup>). Let us define a convex hull spanned over the endmembers  $\mathbf{m}_1, \dots, \mathbf{m}_k$  as

$$M = \left\{ \mathbf{x} : \mathbf{x} = \sum_{j=1}^k a_j \mathbf{m}_j, \quad a_j \geq 0, \quad \sum_{j=1}^k a_j = 1 \right\} \quad (3)$$

In hyperspectral data,  $k$  is usually smaller than the space dimensionality  $p$ , and the endmembers  $\mathbf{m}_1, \dots, \mathbf{m}_k$  are linearly independent. In that case,  $M$  is a  $(k-1)$  dimensional simplex. Define a projection of spectra  $\mathbf{x}$  onto  $M$  as a vector  $\mathbf{x}_M \in M$  such that

$$d(\mathbf{x}, \mathbf{x}_M) = \min \{ d(\mathbf{x}, \mathbf{z}), \mathbf{z} \in M \},$$

where  $d(\cdot, \cdot)$  is a distance between two vectors (points) in a  $p$ -dimensional space. A distance between  $\mathbf{x}$  and  $M$  can now be defined as

$$d(\mathbf{x}, M) = d(\mathbf{x}, \mathbf{x}_M).$$

Here, we will consider the case when  $d(\cdot, \cdot)$  is a Euclidian distance, that is,

$$d(\mathbf{x}, \mathbf{y}) = \sqrt{(\mathbf{x} - \mathbf{y})'(\mathbf{x} - \mathbf{y})}.$$

Once the endmembers  $\mathbf{m}_1, \dots, \mathbf{m}_k$  are defined, the coefficients  $a_{ij}$  can be estimated using the least squares method under the constraints (2), which is equivalent to projecting on the simplex (3) as described above.

Other distances can also be considered. For instance, when the noise in the image is known and its magnitude is large, a suitable distance might be a statistical (Mahalanobis) distance. More research is needed to investigate which distance is more appropriate in a given case.

In order to adjust for dimensionality, we define an adjusted distance as

$$d_{adj}(\mathbf{x}, \mathbf{y}) = \frac{d(\mathbf{x}, \mathbf{y})}{\sqrt{p}}.$$

Since all of our numerical calculations are performed in the same  $p$ -dimensional space, this dimensionality adjustment is not really significant here. However, it makes it easier to interpret the numerical results. Please note that for two spectra differing by a shift of only one unit (up or down), the adjusted distance between the two spectra is equal to one unit (independent of dimensionality (number of spectral bands) used). The adjusted distance is also called a root mean squared error by some authors (e.g., see <sup>7</sup> and <sup>8</sup>).

We now briefly describe the MaxD endmember selection techniques, which will be used as a comparison with the Simplex Projection Methods (see Section 3 for the definition). We will also use the well known Pixel Purity Index (PPI) method (its description can be found in <sup>1</sup> and <sup>4</sup>, for example).

The Maximum Distance (MaxD) method starts with identifying two extreme spectra and then orthogonally projecting (along the line connecting the two extreme points) all image spectra into a lower dimensional subspace. As a result, the two extreme points collapse into one point. Then we find a spectrum that is farthest from the collapsed point and identify this spectrum as the next endmember. The projections are then continued (along the line connecting the new endmember and the collapsed point) until the desired number of endmembers is identified. More details are given in <sup>3</sup> (and also in <sup>1</sup>).

### 3. SIMPLEX PROJECTION METHODS (SPM)

Since our emphasis is on having small adjusted distances  $d_{adj}(\mathbf{x}_i, M_k)$ , it makes sense to consider a summary measure of those adjusted distances and then to minimize it by the appropriate choice of endmembers. Examples of summary measures could be the mean, a high percentage (e.g., 99.5%) quantile (percentile), or a maximum value (these and other summary measures are discussed in Section 4). Since it would not be feasible to check all possible sets of spectra as endmembers, we need to rely on some heuristic procedures to minimize a summary measure. Natural choices in this case would be some forward, backward, or stepwise procedures. When using these procedures, we find that direct optimization of a chosen criterion would still be very computationally intensive. So, instead of directly optimizing a summary measure, we optimize a choice of a single endmember at each step by investigating its projection on a simplex generated by other endmembers. We call such algorithms Simplex Projection Methods (SPMs). The SPMs should lead to (but do not guarantee) better values of the summary measures.

We consider two examples of SPMs—a forward method that we call the Farthest Pixel Selection (FPS) method (introduced in <sup>16</sup>) and a stepwise method that we call the Stepwise Simplex Projection (SSP) method.

#### 3.1. Farthest Pixel Selection (FPS) Method

The Farthest Pixel Selection (FPS) method is defined as follows:

1. Select the longest spectra vector as  $\mathbf{m}_1$  (first endmember).
2. Select the spectra farthest from  $\mathbf{m}_1$  as  $\mathbf{m}_2$ . Set  $k = 2$ .
3. Define  $M_k$  according to (3), and select the spectra farthest from  $M_k$  as  $\mathbf{m}_{k+1}$ . Increase the value of  $k$  by 1.
4. Repeat step 3 until the desired number of endmembers is selected.

The FPS method is very similar to the Unsupervised FCLS (Fully Constrained Least Squares) introduced in <sup>5</sup> in terms of the resulting endmembers, assuming that the value of  $\delta$  used in <sup>5</sup> is chosen appropriately ( $\delta = 10^{-5}$  for the data set used here). The main difference is that we use this method only to identify endmembers, and then, for the purpose of target detection, we use only one detector (matched subspace detector) for all endmember selection techniques because our main goal is to investigate a wide range of these techniques without the confounding effect of the target detection method. On the other hand, in <sup>5</sup>, the emphasis is on material quantification based on estimates of the abundance coefficients  $a_{ij}$  in the model (1), and the detection is based on the magnitude of the abundances.

Note that all of the three endmember selection methods discussed so far (MaxD, PPI, and FPS) are what we could call sequential methods. That is, a new endmember is added to the previous  $k$  endmembers to form a set of  $(k+1)$  endmembers. Some other endmember selection techniques may not be sequential. For example, the N-FINDR algorithm (searching for the maximum volume simplex with vertices at selected image spectra; see [12]) does not have this property. The SSP method discussed in the next section is not sequential as well.

### 3.2. Stepwise Simplex Projection (SSP) Method

The Stepwise Simplex Projection (SSP) method is similar to FPS. However, at each step we check if one of the previously chosen endmembers is suboptimal in the sense that it is close to the simplex created by all other endmembers. In FPS, when a spectrum is chosen as an endmember, it is far from the simplex generated by previous endmembers, so it is usually an important addition. However, adding more endmembers may sometimes make a given endmember “obsolete,” that is, less important than other endmembers. The SSP method is defined as follows:

1. Select the longest spectra vector as  $\mathbf{m}_1$  (first endmember).
2. Select the spectra farthest from  $\mathbf{m}_1$  as  $\mathbf{m}_2$ . Set  $k = 2$ .
3. Define  $M_k$  according to (3), and select the spectra farthest from  $M_k$  as  $\mathbf{m}_{k+1}$ . This results in  $M_{k+1}$  generated by  $(k+1)$  endmembers.
4. For each of the  $(k+1)$  endmembers generating  $M_{k+1}$ , calculate its distance  $d_j$ ,  $j=1, \dots, (k+1)$  to the simplex generated by the remaining  $k$  endmembers. The distance  $d_{k+1}$  was already calculated in the previous step.
5. If  $\min\{d_j : 1 \leq j \leq k\} \geq d_{k+1}$ , increase the value of  $k$  by 1, and continue with Step 3 using the endmembers identified so far. Otherwise (when  $\min\{d_j : 1 \leq j \leq k\} < d_{k+1}$ ), eliminate the endmember with the smallest distance  $d_i$ , and continue with Step 3 using the remaining endmembers.
6. Repeat Steps 3 to 5 until the desired number of endmembers is selected.

The SSP method is not sequential because some of the previously chosen endmembers can be eliminated in Step 5.

### 3.3. Numerical Methods

In order to find the projection  $\mathbf{x}_M$  of a given spectra  $\mathbf{x}$ , we need to minimize the distance  $d(\mathbf{x}, \sum_{j=1}^k a_j \mathbf{m}_j)$  given the constraints  $a_j \geq 0, \sum_{j=1}^k a_j = 1$ . The square of the distance can be written as

$$d^2\left(\mathbf{x}, \sum_{j=1}^k a_j \mathbf{m}_j\right) = \mathbf{x}^T \mathbf{x} - \mathbf{v}^T \mathbf{a} + \mathbf{a}^T \mathbf{Q} \mathbf{a}$$

where  $\mathbf{a}^T = [a_1, \dots, a_k]$ ,  $\mathbf{v}^T = 2\mathbf{x}^T \mathbf{B}$ ,  $\mathbf{Q} = \mathbf{B}^T \mathbf{B}$ , and  $\mathbf{B}$  is the matrix of endmembers  $\mathbf{m}_1, \dots, \mathbf{m}_k$  as columns. So, the minimization problem becomes a quadratic programming problem. In order to deal with the equality constraint  $\sum_{j=1}^k a_j = 1$ , the authors in <sup>5</sup> introduce a constant  $\delta$  (see formulas (17) and (18) in <sup>5</sup>). However, precision of results depends on the appropriate choice of  $\delta$ , which is rather inconvenient. Our approach is to eliminate  $a_k$  and introduce a new constraint  $\sum_{j=1}^{k-1} a_j \leq 1$ . The numerical results are obtained using the S-plus function “solve.QP” for quadratic programming.<sup>6</sup> When using the method employed in <sup>5</sup>, a reasonable precision is obtained for  $\delta = 10^{-5}$  in our numerical examples.

## 4. SUMMARY MEASURES FOR SIMPLEXES

In <sup>16</sup>, we were using histograms to investigate the magnitude of the approximation errors in (1). A disadvantage of such an approach is that a whole graph is needed to summarize the goodness of approximation for a given set of

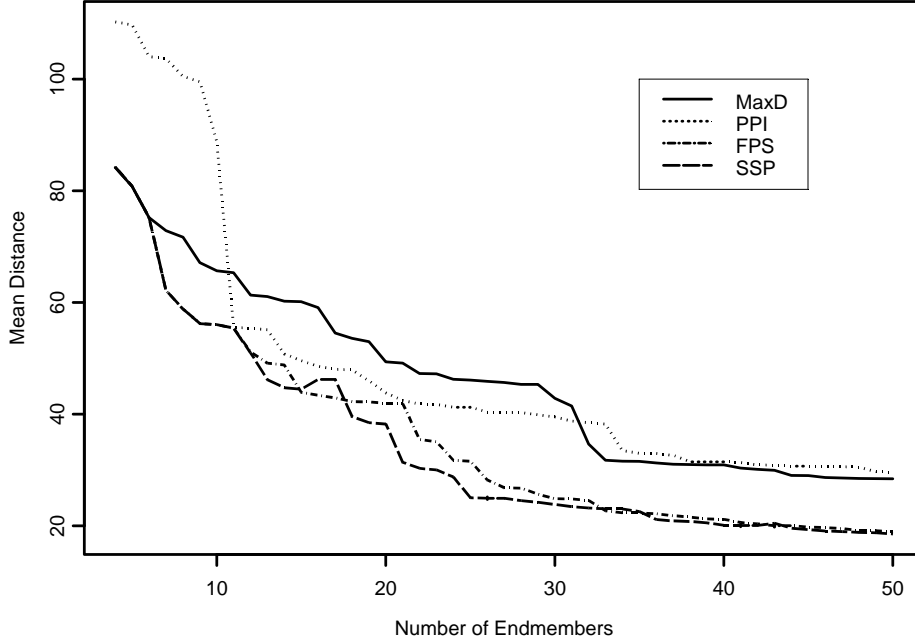


Figure 1. Mean Distance (MD) as a function of the number (ranging from 4 to 50) of endmembers in the MaxD (solid line), PPI (dotted line), FPS (dotted-dashed line), and SSP (dashed line) simplexes.

endmembers. In order to investigate how this approximation depends on the number of endmembers and the method to generate the endmembers, it is convenient to consider summary measures of the approximation errors. We discuss and investigate the following four summary measures:

- Mean Distance (MD)
- Root Mean Squared Distance (RMSD)
- Maximum
- Percentile.

#### 4.1. Mean Distance (MD)

The Mean Distance (MD) is defined as the average of adjusted distances, that is,

$$MD\{M\} = \frac{1}{n} \sum_{i=1}^n d_{adj}(\mathbf{x}_i, \mathbf{x}_{iM})$$

where  $\mathbf{x}_{iM}$  is a projection of  $\mathbf{x}_i$  onto the simplex  $M$ , as defined previously.

Figure 1 shows that the two simplex projection methods are not much different as measured by MD, and they both are performing better than the two remaining methods. A disadvantage of MD as a measure of the approximation errors is that it may be insensitive to a relatively small fraction of spectra with large approximation errors. In subpixel target detection, we are often interested in a relatively small number of pixels (that contain the target), and we want to make sure that a significant majority of pixel spectra (or, even better, all of them) are well approximated in formula (1). To address this issue, we introduce another measure in the next subsection.

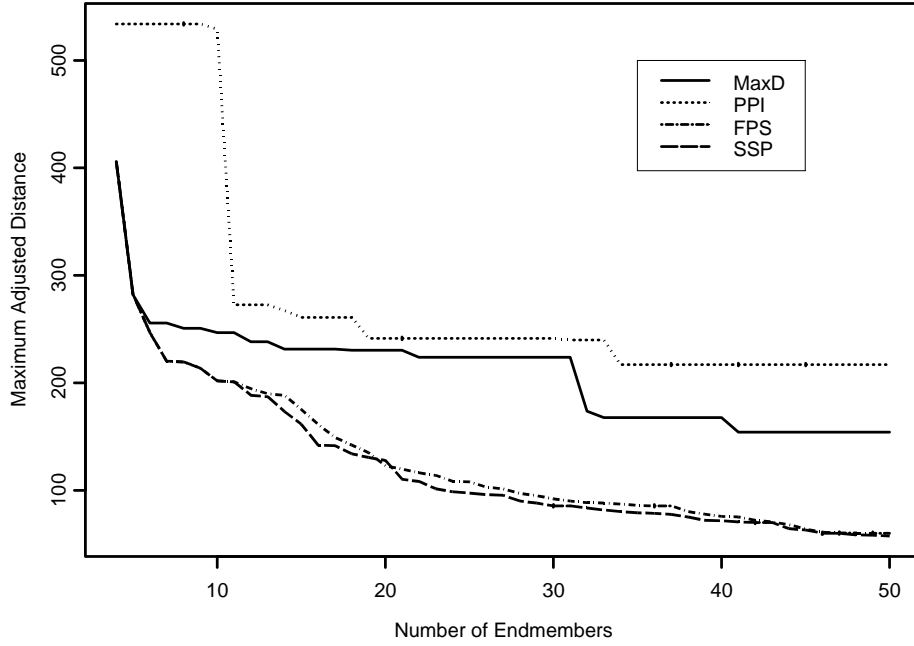


Figure 2. The maximum adjusted distance as a function of the number (ranging from 4 to 50) of endmembers in the MaxD (solid line), PPI (dotted line), FPS (dotted-dashed line), and SSP (dashed line) simplexes.

## 4.2. Root Mean Squared Distance (RMSD)

The RMSD is defined as

$$RMSD\{M\} = \sqrt{\frac{1}{n} \sum_{i=1}^n [d_{adj}(\mathbf{x}_i, \mathbf{x}_{iM})]^2}$$

The RMSD is more sensitive than MD to large distances because the distances are squared. However, when only a small fraction of pixels has larger distances, this sensitivity may not have a significant impact on RMSD. This turns out to be the case for our numerical example, and a plot of RMSD for all four methods is very similar to Figure 1 and is not shown here.

## 4.3. Maximum Distance

Both previous measures are based on averaging over the whole set of the image pixels. Since even small images usually have at least 10,000 pixels, the impact of a small fraction of pixels may be unnoticed when those measures are used. This is why it might be informative to use the maximum of the adjusted distances, that is,

$$\max \{d_{adj}(\mathbf{x}_i, \mathbf{x}_{iM}) : 1 \leq i \leq k\}$$

Figure 2 shows the relationship among the four methods to be somewhat similar to that shown in Figure 1. One difference is that the PPI performs much worse when the maximum distance measure is used.

The maximum adjusted distance may seem to be sensitive to the presence of outliers. As with any data, extreme outliers should be investigated. If they are a result of an error, then they can be removed. However, in practice it is often difficult or impractical to make a decision about removing an outlier. An extreme outlier would most likely be identified as one of the endmembers. In that case, the adjusted distance of the outlying spectra to the endmember simplex would be zero, which would not interfere with any of the simplex measures defined here. Another issue is the impact of the outlier identified as an endmember on the target detection performance, which is discussed in the section on target detection.

The maximum adjusted distance used as a measure of approximation in (1) takes into account only the most extreme spectrum. One could argue that we are not very much concerned about a single spectrum in the whole image. To overcome this difficulty, we introduce one more measure in the next subsection.

#### 4.4. Percentile (Quantile)

When we are concerned about a very small fraction of the image pixels, we can use a high percentile, for example, the 99.9 percentile of adjusted distances. This gives an adjusted distance such that only 0.1 percent of the image spectra (in our AVIRIS image, this means 10 spectra) are even farther from the endmember simplex. A plot of the 99.9 percentile of adjusted distances for all four methods is very similar to Figure 2 and is not shown here.

#### 4.5. Conclusions on Summary Measures

For the AVIRIS data set used here, all four summary measures show similar relationships among the investigated endmember selection techniques. This strengthens the final conclusions about these relationships. We advocate using at least three of these summary measures in practice. The RMSD should be used to assess overall “goodness-of-fit” (with some penalty for very large approximation errors). The maximum distance and a high percentile should be used to evaluate whether the endmembers give a good approximation in (1) for all (or almost all) pixels.

### 5. SUBPIXEL TARGET DETECTION

For the purpose of sub-pixel target detection, we use a geometric approach that leads to structured models. An overview of target detection approaches and their classification has been published throughout the literature (e.g., <sup>9</sup> and <sup>10</sup>, and especially the monograph <sup>11</sup>). In this paper, we use only one simple detector (a matched subspace detector (MSD)) in order to simplify the process of comparison of the endmember selection techniques.

The target of interest was a reddish-brown paint used on basketball and tennis court playing surfaces. From the 100 by 100 image, one pixel was identified as a fully resolved pixel of the reddish-brown paint, and its spectrum was defined as the target spectrum. Our goal was to detect the target spectra in the remaining 9,999 pixels. From prior research,<sup>1</sup> we know that 13 pixels (out of 9,999) contain the target spectra. This approach is not as realistic as the invariant approach used in <sup>1</sup>. However, it is simpler, and it allows a comparison of several endmember selection methods for the background without confounding their effect with the modeling of the target region.

It is now convenient to write the linear mixing model (1) in a form more suitable for target detection. That is, we are now assuming the following structured model:

$$\mathbf{x}_i = \mathbf{t} \cdot a_i + \mathbf{B} \cdot \mathbf{b}_i + \boldsymbol{\varepsilon}_i \quad (4)$$

where  $\mathbf{t}$  is a fixed vector of the target spectrum,  $\mathbf{B}$  is a fixed matrix of background endmembers as columns, and  $a_i$ ,  $\mathbf{b}_i$  are unknown constant and vector, respectively. All target detection in this paper is done using a matched subspace detector (MSD):

$$MSD(\mathbf{x}) = \frac{\mathbf{x}^T (\mathbf{P}_Z - \mathbf{P}_B) \mathbf{x}}{\mathbf{x}^T (\mathbf{I} - \mathbf{P}_Z) \mathbf{x}}$$

where  $\mathbf{I}$  is the identity matrix,  $\mathbf{Z} = [\mathbf{t} \ \mathbf{B}]$  is a matrix consisting of  $\mathbf{t}$  as the first column and then all columns of  $\mathbf{B}$ , and  $\mathbf{P}_Y$  (for  $\mathbf{Y}$  equal to  $\mathbf{B}$  or  $\mathbf{Z}$ ) is the matrix of the projection onto the space generated by columns of  $\mathbf{Y}$ , that is,

$$\mathbf{P}_Y = \mathbf{Y} (\mathbf{Y}^T \mathbf{Y})^{-1} \mathbf{Y}^T .$$

In this section, the background endmembers needed as columns of the matrix  $\mathbf{B}$  in formula (4) are identified as follows. A set of  $n = 10,000$  spectra consists of all pixels in the 100 by 100 image. This includes one target spectrum (based on the fully resolved target pixel) and the 9,999 image pixel spectra that are not identical with the target spectrum. First, one of the investigated endmember selection techniques is applied to all  $n = 10,000$  spectra in order to find a given number of  $k$  endmembers. If the target spectrum is among those endmembers (which is usually the case for sufficiently large  $k$ ), then it is removed, and the remaining endmembers are used as columns in the matrix  $\mathbf{B}$ .

### 5.1. Metrics for Evaluation of Target Detection Methods

We evaluate target detection performance based on the observed ROC curves. An observed ROC curve is a plot of detection rate (DR) versus false alarm rate (FAR). We specifically use the term “detection rate” rather than “probability of detection” because these results are based on the observed frequency of detecting the target rather than on theoretical calculations of probabilities.

In this type of study, we usually want to consider a large number of cases, for example, several endmember selection methods and several numbers of endmembers to be chosen. To investigate a large number of cases, several summary metrics were developed in <sup>1</sup>. We use some of those summary metrics in this paper. Specifically, we use the Average FAR (AFAR) in addition to summarizing detection rates (DR) at a fixed FAR level. In order to define AFAR, let us assume that there are  $m$  image pixels that contain the target. The observed ROC curve is fully described by  $m$  numbers  $r_i, i = 1, \dots, m$ , where  $r_i$  is the lowest FAR to achieve  $i/m$  detection rate (DR). The AFAR is defined as

$$AFAR = \frac{1}{m} \sum_{i=1}^m r_i$$

If the observed ROC curve is plotted as a step function

$$ROC(x) = \max \{i/m : r_i \leq x\}, \text{ for } 0 \leq x \leq 1,$$

then AFAR is the area above the observed ROC curve (to be more precise, the area between the observed ROC curve and the DR level of 1). Consequently, AFAR can also be expressed as one minus the area under the observed ROC curve.

### 5.2. Singular Value Decomposition (SVD)

So far in this paper, we were using endmembers to characterize the image spectra through the model (4). However, for the purpose of target detection, the background vectors in the matrix  $\mathbf{B}$  in the model (4) do not necessarily have to represent spectra of actual materials (in that case we call the vectors “basis vectors” rather than endmembers). By this terminology, any of the endmembers can be used as basis vectors, but not all basis vectors are endmembers. The use of basis vectors that do not represent any material spectra causes problems with interpretation of the model (4) in terms of the linear mixing model. On the other hand, such basis vectors may be acceptable as long as they lead to reasonable target detection.

A popular method to generate basis vectors that are not endmembers is the Singular Value Decomposition (SVD) technique used in <sup>15</sup>. Let us define a  $p \times n$  matrix  $\mathbf{Y}$  of all background spectra  $\mathbf{x}_i$  (given as columns). In our example,  $n = 9,999$  because we need to remove the target spectrum. Consider the singular value decomposition (SVD) of  $\mathbf{Y}$ :

$$\mathbf{Y} = \mathbf{U}\mathbf{D}\mathbf{V}^T$$

where  $\mathbf{U}_{p \times p} = [u_j]_{j=1, \dots, p}$  is the matrix of eigenvectors of  $\mathbf{Y}\mathbf{Y}^T$  and  $\mathbf{D}$  is the diagonal matrix of singular values such that  $\sigma_1 \geq \sigma_2 \geq \dots \geq \sigma_p \geq 0$ . The SVD technique uses the first  $r$  columns of  $\mathbf{U}$ , that is,  $\mathbf{B} = [u_1, \dots, u_r]$ , as the background basis vectors.

### 5.3. AFAR Results

Figure 3 shows the AFAR values for the MSD used with a specified number of background basis vectors (ranging from 4 to 49) generated by four endmember selection techniques and the SVD method. Using fewer than four basis vectors produces much higher AFAR values, so those cases are not plotted. The SVD is a preferred method for up to 8 background basis vectors. When between 9 and 25 background basis vectors are used, one of the two simplex projection methods (alternatively, FPS or SSP) is the best of the five methods. For 26 to 29 background basis vectors, the SVD is the best method, but unfortunately it performs much worse in the range of 9 to 25 background basis vectors.

In general, we prefer methods that give consistently good results in a wide range of the number of background basis vectors, because in practice, we do not know how to identify the optimum number of background basis vectors for a given image with unknown target pixels.

Figure 3 shows that using more than 35 background basis vectors is not beneficial for any of the five methods investigated. However, when we do use that many background basis vectors, the SSP and PPI methods are the best among the five methods.

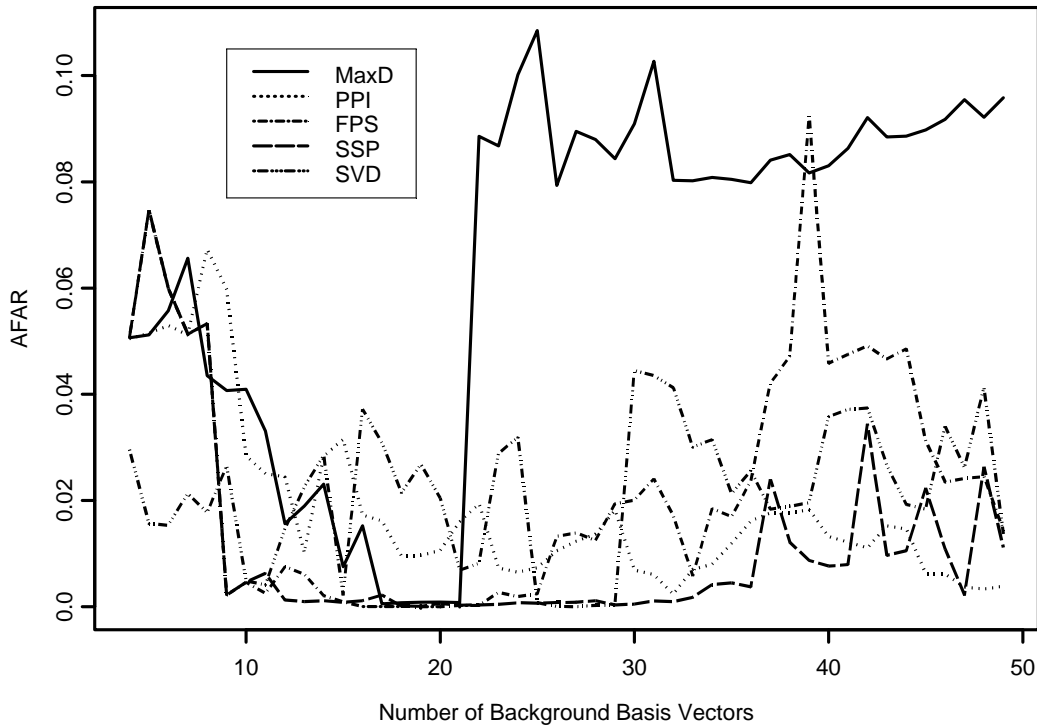


Figure 3. The AFAR as a function of the number (ranging from 4 to 49) of basis vectors generated by the MaxD (solid line), PPI (dotted line), FPS (dotted-dashed line), SSP (dashed line), and SVD (multidotted-dashed line) methods.

Note the poor performance of MaxD for 22 or more background basis vectors. The reason is that the 22nd endmember identified by MaxD turns out to be one of the 13 mixed-target pixels. This clear failure of the MaxD method means that the MSD detector is not well defined because both the numerator and denominator are zero. However, we can assume that  $r_m = 1$ , which means that the last target is not detected until all non-target pixels are identified as targets. Consequently, the AFAR values are very large in that case.

Identifying one of the mixed target pixels as the background endmember is a serious problem, and it is a potential disadvantage of the native endmember selection techniques. It can happen when the target material is mixed with a background material that is not present as a fully resolved pixel in the image. The non-native endmember selection techniques (for examples see <sup>13</sup> and <sup>14</sup>) and basis vector selection techniques such as SVD are unlikely to encounter this type of problem. However, this does not mean that they necessarily perform better as target detectors.

Table I shows the optimum performance of each of the five methods. The SVD gives the best (the smallest) AFAR value; however, it is not as consistent (for a range of the number of background basis vectors) as the two simplex projection methods, especially SSP (as seen in Figure 3).

TABLE I  
BEST (SMALLEST) AFAR VALUES ( $\cdot 10^4$ ) FOR DETECTION OF ALL 13 TARGET PIXELS FOR UP TO 49 BACKGROUND BASIS VECTORS. NEXT TO EACH AFAR ENTRY (IN PARENTHESES) ARE THE NUMBER OF BACKGROUND BASIS VECTORS USED TO ACHIEVE THE PRESENTED AFAR VALUE.

Background Basis Vector Selection Method				
MaxD	PPI	FPS	SSP	SVD
5.62 (17)	23.54 (32)	0.31 (19)	1.00 (19)	.15 (27)

In order to measure the consistency of the five investigated methods, we can calculate averages over a specific range of the number of background basis vectors. Based on Figure 3, we conclude that a reasonable range for most methods is between 10 and 35 background basis vectors. Table II shows the AFAR values averaged over that range and multiplied by  $10^4$ .

TABLE II  
THE AFAR VALUES ( $\cdot 10^4$ ) AVERAGED OVER THE NUMBER OF BACKGROUND BASIS VECTORS FROM 10 TO 35.

Background Basis Vector Selection Method				
MaxD	PPI	FPS	SSP	SVD
538	140	74	15	193

Overall, we recommend the SSP method as the most consistent among the five investigated methods.

#### 5.4. Detection Rates

Figure 4 shows detection rates when assuming only five false alarms among 9986 non-target pixels (approximately  $5 \cdot 10^{-4}$  FAR). The results are not as discriminating among the methods as those for the AFAR results due to the discrete nature of detection rates for only 13 target pixels. The best performance (reaching over 0.9 detection rate) is observed for the FPS method at 16 to 22 background basis vectors and the SVD method for 26 and 27 background basis vectors.

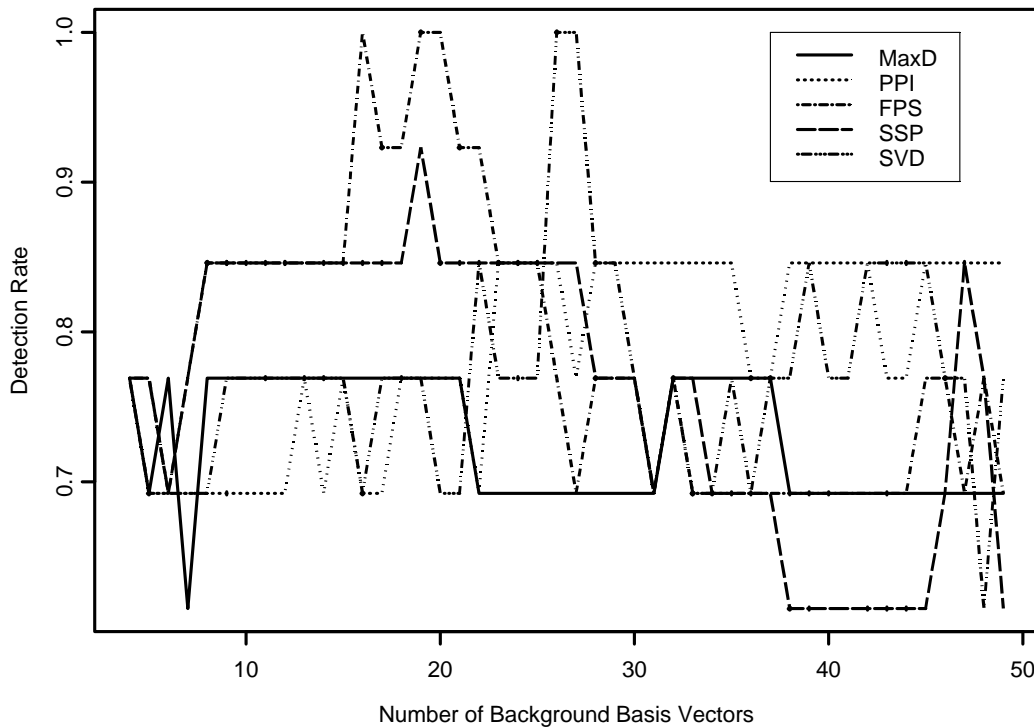


Figure 4. Detection rate as a function of the number (ranging from 4 to 49) of basis vectors generated by the MaxD (solid line), PPI (dotted line), FPS (dotted-dashed line), SSP (dashed line), and SVD (multidotted-dashed line) methods.

Calculations of detection rates at other FAR levels (we used  $10^{-4}$  and  $10^{-3}$  FAR) show relationships among the five investigated methods similar to those shown in Figure 4. A disadvantage of Figure 4 is that many lines overlap each other, and it is difficult to trace performance of a specific method. At the same time, in practice, we do not know the optimum number of background basis vectors, and we are interested in consistency over a range of background basis vectors. Again, it is useful to calculate the average over a range of the number of background basis vectors. Figure 4 shows again that the range between 10 and 35 of background basis vectors gives reasonable performance for all methods. Table III shows the average values in that range for three levels of FAR and all 5 methods investigated here.

TABLE III  
AVERAGE DETECTION RATES OVER THE RANGE FROM 10 TO 35 OF BACKGROUND BASIS VECTORS FOR ALL 5 METHODS AND THREE FAR LEVELS.

FAR level	Background Basis Vector Selection Method				
	MaxD	PPI	FPS	SSP	SVD
$10^{-4}$	0.734	0.666	0.799	0.760	0.719
$5 \cdot 10^{-4}$	0.740	0.784	0.831	0.817	0.778
$10^{-3}$	0.760	0.796	0.846	0.855	0.805

All detection rates in Table III are very close to each other. This indicates no major differences among the five investigated methods, when the optimum number of basis vectors is unknown. The FPS and SSP methods are slightly better than the remaining methods.

### 5.5. Conclusions on Target Detection

Based on the results in this paper and in <sup>1</sup>, it is clear that the detector's performance is highly dependent on the number of basis vectors and the method used to generate those basis vectors. It would be beneficial to know the optimum number of basis vectors for a given image data and the method used. However, in practice we do not know that optimum number, so we need to use methods that are consistently good over wide ranges of the number of basis vectors. Both simplex projection methods discussed in this paper are performing quite well in this regard. More research is needed to see if similar behavior is observed for other hyperspectral images and other detectors.

## 6. OVERALL CONCLUSIONS AND FUTURE WORK

There is a prevailing perception in the current literature that a relatively small set of endmembers (from 5 to 10) can be used to describe an image through a linear mixing model (1). Our numerical results indicate that the resulting approximation may not be sufficient for many applications. We observe significant differences between the observed spectra and the modeled spectra (convex linear combinations of endmembers), even for as many as 20 or 40 endmembers (depending on the method used). In order to find endmembers that more closely estimate the image spectra, we introduce a family of simplex projection methods and investigate two examples from that family (FPS and SSP methods). Both simplex projection methods show promising performance, but still a relatively large number of endmembers is needed to obtain reasonably good approximations of all image pixels.

Further work is needed to see if the conclusions from this research also apply to

- other important detectors (especially those discussed in <sup>11</sup>), and
- other hyperspectral images.

Future work may also include investigation of other types of simplex projection methods.

### Acknowledgment

The author would like to thank Professor John Schott and Emmett Ientilucci for helpful discussions and suggestions regarding this paper. This work was partially funded under the Office of Naval Research Multi-disciplinary University Research Initiative "Model-based Hyperspectral Exploitation Algorithm Development" #N00014-01-1-0867.

### References

- [1] P. Bajorski, J. Schott, and E. Ientilucci. "Comparison of Basis-Vector Selection Methods for Target and Background Subspaces as Applied to Subpixel Target Detection" *Proc. SPIE, Algorithms and Technologies for Multispectral, Hyperspectral, and Ultraspectral Imagery X*, Orlando, FL, April 2004, pp. 97-108.

- [2] A. R. Gillespie, Smith, M. O., Adams, J. B., Willis, S. C., Fischer, A. F., and Sabol, D. E.. "Interpretation of residual images: spectral mixture analysis of AVIRIS images," Owens Valley, California. In Proc. 2nd Airborne Visible/Infrared Imaging Spectrometer (AVIRIS) Workshop (R. Green, Ed.), Pasadena, CA, 4-5 June, 1990, JPL Publication 90-54, Jet Propulsion Laboratory, Pasadena, CA, pp. 243-270.
- [3] J. R. Schott, K. Lee, R. Raqueno, G. Hoffmann, and G. Healey. "A subpixel target detection technique based on the invariance approach." To be published, 2004.
- [4] J. W. Boardman, F. A. Kruse, and R. O. Green. Mapping target signatures via partial unmixing of AVIRIS data. In Fifth JPL Airborne Earth Science Workshop, volume 1 of JPL Publication 95-1, pp. 23-26, 1995.
- [5] D. C. Heinz and C-I Chang, "Fully Constrained Least Squares Linear Spectral Mixture Analysis Method for Material Quantification in Hyperspectral Imagery," *IEEE Transactions on Geoscience and Remote Sensing*, Vol. 39, No. 3, pp. 529-545, March 2001.
- [6] B.A.Turlach <http://www.maths.uwa.edu.au/~berwin/software/quadprog.html> (last accessed on 11/26/04).
- [7] T. H. Painter, J. Dozier, D. A. Roberts, R E. Davis, R. O. Green (2003). "Retrieval of subpixel snow-covered area and grain size from imaging spectrometer data." *Remote Sensing of Environment*, 85, pp. 64-77.
- [8] Painter, T. H., Roberts, D. A., Green, R. O., & Dozier, J. (1998). The effect of grain size on spectral mixture analysis of snow-covered area from AVIRIS data. *Remote Sensing of Environment*, 65(3), 320-332.
- [9] D. Manolakis. Overview of algorithms for hyperspectral target detection: theory and practice. *Proc. SPIE Algorithms and Technologies for Multispectral, Hyperspectral, and Ultraspectral Imagery VIII*, volume 4725, pp. 202-251, Orlando, FL, April 2002.
- [10] D. Manolakis and G. Shaw. Detection algorithms for hyperspectral imaging applications. *IEEE Signal Processing Magazine*, 19 (1):29-43, January 2002.
- [11] Chein-I Chang, *Hyperspectral Imaging: Techniques for Spectral Detection and Classification*, Kluwer Academic/Plenum Publishers, 2003.
- [12] Winter, Michael E., "N-FINDR: an Algorithm for Fast Autonomous Spectral End-member Determination in Hyperspectral Data", *Proc. of SPIE Vol 3753, Imaging Spectrometry V (Descour and Shen, editors)*, pp. 266 -277, 1999.
- [13] M. Craig, "Minimum-volume transforms for remotely sensed data," *IEEE Transactions on Geoscience and Remote Sensing*, vol. 32, pp. 542-552, 1994.
- [14] M. Berman, H. Kiiveri, R. Lagerstrom, A. Ernst, R. Dunne, and J. Huntington. "ICE: An automated statistical approach to identifying endmembers." In *Proc. 2003 IEEE International Geoscience and Remote Sensing Symposium*, Volume 1, Toulouse, France, pp. 279-283, July 2003.
- [15] G. Healey and D. Slater, "Models and methods for automated material identification in hyperspectral imagery acquired under unknown illumination and atmospheric conditions," *IEEE Trans. Geosci. Remote Sensing*, vol. 37(6), pp. 2706-2717, November 1999.
- [16] P. Bajorski, "Simplex Projection Methods for Selection of Endmembers in Hyperspectral Imagery," *Proc. of IEEE International Geoscience and Remote Sensing Symposium, September 2004*.